Scale invariant pattern recognition with logarithmic radial harmonic filters

Joseph Rosen and Joseph Shamir

A generalized approach leads to spatial filters that accept changes of scale by a factor of 4. The procedure employs phase filters with reduced tolerance requirements and achieves high discrimination capability and efficient light throughput. Computer simulations and laboratory experiments show the advantages of this novel approach.

I. Introduction

Conventional methods of optical pattern recognition suffer from the requirement of high-resolution recording materials and distortion sensitivity. In some recent publications[1–3] a new general procedure was introduced that may be employed for generating spatial filters with reduced resolution requirements. Partial and complete rotation invariance was demonstrated in computer simulations and laboratory experiments employing bipolar amplitude filters, phase-only filters, and composite phase filters.

The treatment of scale changes is more involved than rotation since rotation is a periodic function while scale may in principle change infinitely. Therefore, while complete rotation invariance is possible scale changes must be limited within certain ranges.

Previous attempts for scale invariant pattern recognition involved pretransformations,[4] wavelength scanning,[5] and filter multiplexing.[6–9] In this work we introduce a logarithmic radial harmonic (LRH) transformation to implement scale invariant filtering. The initial goal of our research project,[1] the application of reduced information content filters, is preserved together with object shift invariance and a high degree of scale invariance compared to previous attempts. For more general distortion invariance this filter has the advantage over rotation invariant filters since it can be easily combined with mechanical or electronic rotation to yield a system with rotation and scale invariance maintaining the intrinsic shift invariance of Fourier plane processors.

II. Logarithmic Radial Harmonic Transform

Using an approach similar to our procedure for rotation invariant filtering with circular harmonic filters as described in Ref. 3, here too we start with the correlation operation

$$C_{ij}(x_0,y_0) = \int f_i(x,y) m_j^*(x - x_0, y - y_0)\,dx\,dy, \tag{1}$$

where $m_j(x,y)$ is some characteristic filter function matched to the input pattern $f_j(x,y)$. We focus our attention on the value of the correlation function at the origin that reduces to the inner product of f_i and m_j,

$$C_{ij}(0,0) = \int f_i(x,y) m_j^*(x,y)\,dx\,dy, \tag{2}$$

keeping in mind that the distribution over the whole plane should be considered for efficient pattern recognition.

To treat the subject of rotation and scale variance it is advantageous to convert into polar coordinates with Eq. (3) given now in the form

$$C(0) = \int_0^\infty \int_0^{2\pi} f(r,\theta) m^*(r,\theta) r\,d\theta\,dr. \tag{3}$$

Here and in the following indices are suppressed for convenience whenever possible without causing ambiguities. To represent the response (at the origin) for an object with its scale changed by a factor a and rotated by an angle α we use the notation

$$C(0;a,\alpha) = \int_0^\infty \int_0^{2\pi} f(ar,\theta + \alpha) m^*(r,\theta) r\,d\theta\,dr. \tag{4}$$

For an ideal distortion invariant filter one would like to keep $C(0;a,\alpha)$ constant regardless of the values of a and α. In Ref. 3 and earlier work[10,11] rotation invariance was extensively studied, and here we concentrate only on the effects of scale variation using the shorthand $C(a)$ for the relevant correlation function. Denoting

The authors are with Technion–Israel Institute of Technology, Department of Electrical Engineering, Haifa 32000, Israel.

Received 15 December 1987.
0003-6935/89/020240-05$02.00/0.

by $F(\rho,\phi)$ the Fourier transform (FT) of $f(r,\theta)$ and by $M(\rho,\phi)$ the FT of $m(r,\theta)$, the scale dependent correlation function may be also written in the form

$$C(a) = \int_0^{2\pi}\int_d^R \frac{1}{a^2} F\left(\frac{\rho}{a}, \phi\right) M^*(\rho,\phi)\rho d\rho d\phi, \tag{5}$$

where we took into account the finite size of the filter R. Since previous research indicated improved filter performance with low frequencies removed, these were eliminated here too by a high pass filter of radius d. A change of integration variables to $\tau = \rho/a$ converts the equation into

$$C(a) = \int_0^{2\pi}\int_{d/a}^{R/a} F(\tau,\phi)M^*(a\tau,\phi)\tau d\tau d\phi. \tag{6}$$

The scale parameter has been transferred to the filter function and to the limits of integration. We shall return to this subject in Sec. V while here we attempt to design a filter which yields a correlation function given by

$$C(a) = C_0 \exp[j\sigma(a)]. \tag{7}$$

If $\sigma(a)$ is any real function of a and C_0 is a constant, one obtains scale invariance with regard to power detection.

With the successful applications of phase-only circular-harmonic filters[3] in mind, one is tempted to consider a similar approach for scale invariance. Thus we introduce the phase-only LRH filter function

$$M_p^*(\rho,\phi) = \exp[j\Omega(\phi)](\rho/d)^{jp/w}, \tag{8}$$

where $\Omega(\phi)$ is an angular phase function that carries all the angular information contained in the phase of the object function,

$$\Omega(\phi) = -\arg\left[\int_d^R F(\rho,\phi)\left(\frac{\rho}{d}\right)^{jp/w}\rho d\rho\right]. \tag{9}$$

The parameter p is the LRH frequency and w is a normalization constant defined by

$$w = \frac{1}{2\pi}\ln(R/d). \tag{10}$$

Equation (8) is closely related to the kernel form of the Mellin transform. Substitution of this filter function into Eq. (6) yields the relation

$$C_p(a) = \left(\frac{a}{d}\right)^{jp/w}\int_0^{2\pi}\exp[j\Omega(\phi)]\left[\int_{d/a}^{R/a} F(\tau,\phi)\tau^{jp/w}\tau d\tau\right]d\phi. \tag{11}$$

This relation is identical in form to Eq. (7) except for the modifications of the limits of integration. If we substitute Eq. (9) into Eq. (11) it cancels the phase of the radial integration leading to a real positive quantity for the whole integral when $a = 1$. Thus one may write

$$|C_p(1)| = \int_0^{2\pi}\left|\int_d^R F(\tau,\phi)\tau^{jp/w}\tau d\tau\right| d\phi, \tag{12}$$

where the index p on the correlation function indicates that it depends on this parameter. Unlike the case of circular harmonics decomposition, the filter function is not periodic with ρ; thus p does not have to be an integer. To obtain high correlation peaks one may start the filter design by choosing p to give a maximal correlation in Eq. (12) and then proceed with Eq. (11).

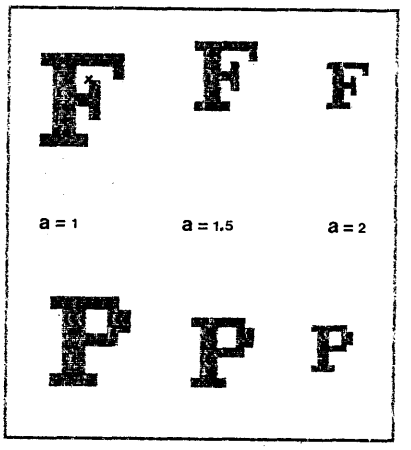

Fig. 1. Input pattern for the computer experiments from which the letter F should be recognized. The x in the large F was the origin for the filter generation, and the scaling factors are as indicated.

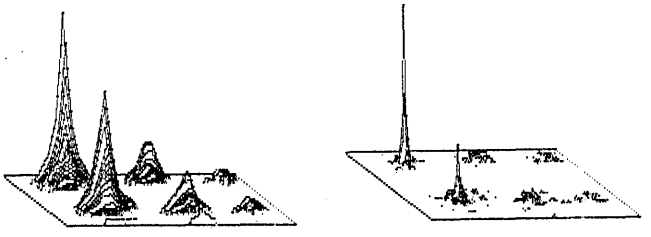

Fig. 2. Output distribution for (a) regular matched filter, (b) phase-only matched filter. The filters were matched to the largest F.

III. Simulation Experiments

The most convenient way to proceed is to invoke a specific example. Previous experiments with block letters indicated that it is most difficult to distinguish between the letters P and F, such as shown in Fig. 1. Thus it is interesting to investigate various filters made to recognize one of these letters against the other. In a computer experiment filters were generated to recognize the letter F from the input pattern of Fig. 1. The performance with a regular matched filter is shown in Fig. 2(a) with the filter matched to the largest F. It is clear that the cross-correlation with P is quite high, much higher than the correlation with the other sizes of F. The autocorrelation peak of a phase-only matched filter is 50 times as high [Fig. 2(b)], but the cross-correlation with P is high too, again much higher than that with the scaled F.

The experimental results shown in Fig. 2 are, respectively, summarized in lines 1 and 2 of Table I with the autocorrelation peak intensity normalized to 1 for the classical matched filter.

To generate a scale invariant filter we return to Eq. (12) and look for the optimal p by plotting the correlation intensity as a function of p (Fig. 3). This plot

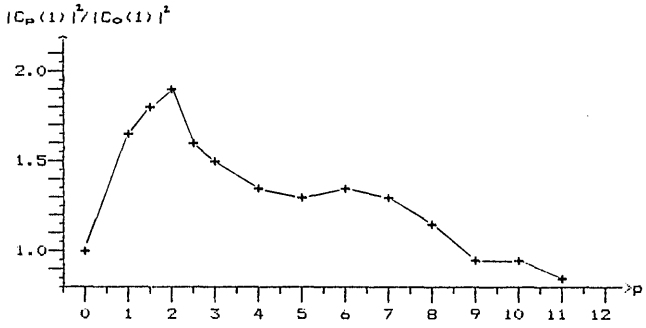

Fig. 3. Correlation peak intensity as a function of the LRH frequency p.

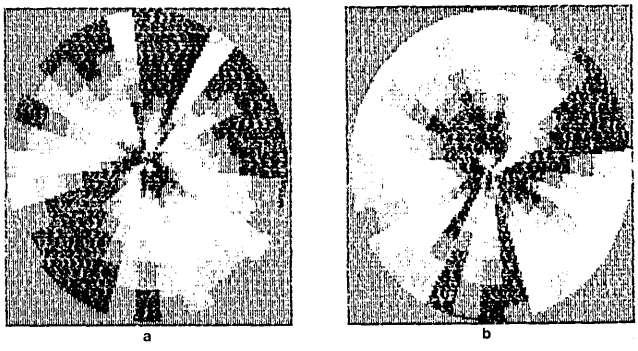

Fig. 4. Real (a) and imaginary (b) parts of the LRH filter represented by four gray levels.

suggests $p = 2$ as a good choice, and with this value we may generate the filter by using Eq. (9). A rough representation of the real and imaginary parts of the filter are shown in Fig. 4, and the output pattern is depicted in Fig. 5. The appropriate correlation values are given in line 3 of Table I.

IV. Laboratory Experiments

To verify the practicability of the new procedure the computer experiments were repeated in the laboratory. We employed the same IBM PC that was used in the simulations to generate the input pattern of Fig. 6 and holographic filter functions like the one shown in Fig. 7. To generate the filters the Fourier plane was sampled into sixty-four rings of equal width and sixty-four angular wedges. The holograms were plotted on a regular dot printer, and the working patterns were obtained by a twenty-five fold photographic reduction onto a regular photographic film. Figure 8 shows the output pattern for a filter made to match the largest F with an intensity scan across the correlation peaks. These results indicate very good performance of the new filters that were implemented with relatively low resolution requirements involving a total of 64 × 64 information elements.

As in the case of circular harmonic filters,[10] here too one has a proper center for which the correlation is optimal. This center may be found by repeating the procedure of filter generation around many points of the object and searching for the one that produces the maximum correlation peak. Naturally this optimal center will be also a function of the parameter p as is the case for the circular harmonics decomposition.

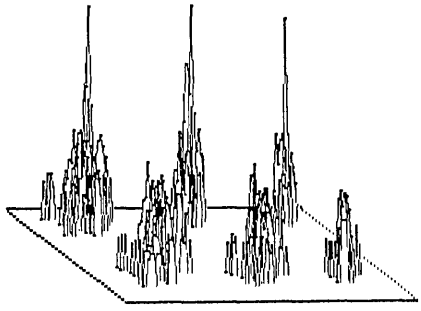

Fig. 5. Output pattern with LRH filter matched to the largest F of the input (Fig. 1).

Table I. Comparison of Performance for the Various Filters Matched to Recognize the Large F

	1	2	3	4
	FILTER	$MAX\{|c(\tau)|^2\}$	$\frac{MAX\{|c(\tau)|^2\}}{MIN\{|c(\tau)|^2\}}$	$\frac{MAX\{|c(\tau)|^2\}}{MAX\{|c(\tau)|^2\}}$
1	MF	1	6	1.5
2	POF	50.8	33.6	2.9
3	RLH-POF (p=2,s=0)	3.8	1.12	2.1
4	RLHF (p=2.0,s=0.05)	2.8	1.03	2.1

Fig. 6. Input pattern for laboratory experiment.

V. Response Equalization

Ideally, the procedure described in this work should lead to a flat system response with regard to scale variance. Unfortunately, due to the finite extent of the spatial filter [the limits of integration in Eq. (11)], the range of the permissible scales is limited, and even in this interval there is some scale dependence. The main contribution to the deterioration of filter performance with the changing scale is the variation of the fraction of the input energy incident within the fixed boundaries of the filter. An additional contribution is due to a filter mismatch that occurs from frequency components that did not participate in the filter generation but come into play as the scale changes. Thus it is clear that no complete scale invariance can be

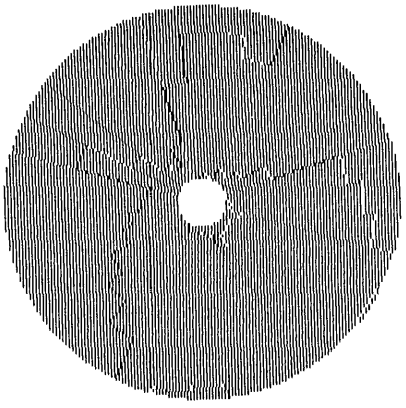

Fig. 7. Holographic LRH filter.

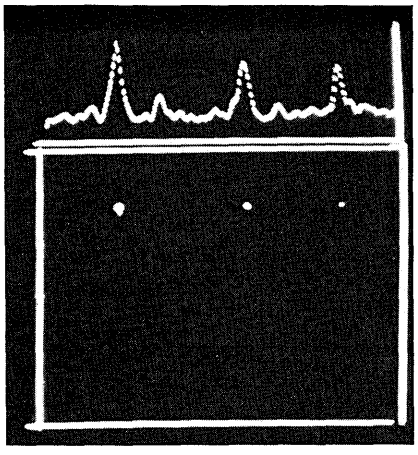

Fig. 8. Output distribution and intensity scan along correlation peaks. Cross-correlations with the P values are invisible due to the threshold chosen.

achieved by this procedure. The scale dependence for the examples analyzed in the previous sections is illustrated in Fig. 9 together with a comparison with the more conventional filters to show the improvement. Experiments indicate a 20% variation of the correlation peak intensity within a range of 4 of the scale factor. Only half of this range is shown in the figure (the region of up to $a = 2$) with a corresponding region (not shown) down to $a = \frac{1}{2}$. To achieve a smaller variation and wider range one may introduce some modifications to the filter function.

Before investigating possible filter modification schemes we introduce a criterion to be used for comparison. A good criterion is defined by the area enclosed between the actual response curve and an ideal flat response:

$$\epsilon = \frac{\int_1^{a_0} ||C(a)| - |C(1)||da}{a_0|C(1)|}, \tag{13}$$

where we defined the range of scale variation between 1 and a_0.

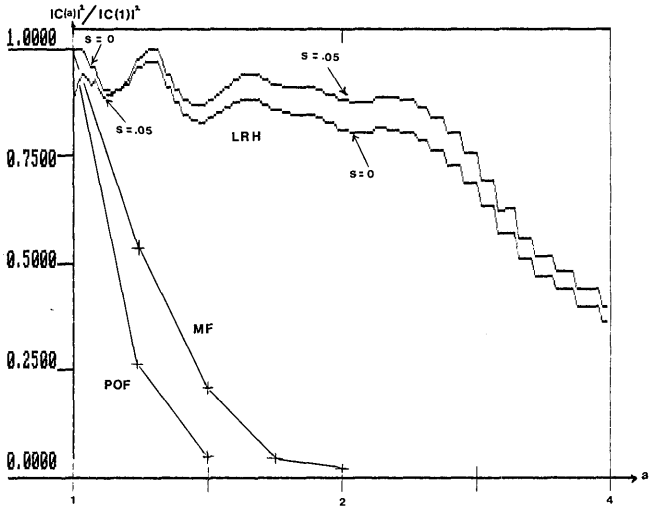

Fig. 9. Scale dependence of correlation peaks normalized to unity. The relative intensities are compared in Table I. MF, matched filter; POF, phase-only matched filter; LRH and modified LRH with $s = 0.05$.

Observation of Fig. 9 indicates a general trend of degradation with increasing a when more of the energy is concentrated in higher spatial frequencies. Thus a straightforward approach toward achieving a flat response is the suppression of low frequencies that correspond to the larger objects by a small amplitude attenuating component in the filter function. This component can be introduced as a small imaginary part of the parameter p in Eq. (8) leading to a modified filter function.

$$M^*(\rho,\phi) = \exp[j\Omega(\phi)](\rho/d)^{s+jp/w}. \tag{14}$$

An optimization procedure led to a minimal ϵ for $s = 0.05$. The performance of a filter designed with this optimal s is summarized in line 4 of Table I and also shown in Fig. 9.

VI. Conclusions

In this work we introduced a new kind of radial transformation to generate scale invariant filters. The superior performance of these filters was demonstrated by computer simulations and laboratory experiments.

The initial goal of the present research project of employing low resolution devices was preserved and demonstrated by using a simple dot printer for the generation of the filters and regular photographic film in the actual experiments.

The laboratory experiments and computer simulations were performed with phase-only filters leading to high throughputs and good pattern distinction. The experiments demonstrated that these filters can operate with a variance of <20% within a scale range of 4. The small residual scale dependence of the correlation peaks can be equalized by several procedures, but these will necessarily lead to a reduction of the correlation peaks.

References

1. J. Shamir, H. J. Caulfield, and J. Rosen, "Pattern Recognition Using Reduced Information Content Filters," Appl. Opt. **26,** 2311 (1987).
2. J. Rosen and J. Shamir, "Distortion Invariant Pattern Recognition with Phase Filters," Appl. Opt. **26,** 2315 (1987).
3. J. Rosen and J. Shamir, "Circular Harmonic Phase Filters for Efficient Rotation-Invariant Pattern Recognition," Appl. Opt. **27,** 2895 (1988).
4. D. Casasent and D. Psaltis, "Position, Rotation, and Scale Invariant Optical Correlation," Appl. Opt. **15,** 1795 (1976).
5. K. Mersereau and G. M. Morris, "Scale, Rotation, and Shift Invariant Image Recognition," Appl. Opt. **25,** 2338 (1986).
6. G. F. Schils and D. W. Sweeney, "Iterative Technique for the Synthesis of Distortion-Invariant Optical-Correlation Filters," Opt. Lett. **12,** 307 (1987).
7. T. Szoplik, "Shift and Scale-Invariant Anamorphic Fourier Correlator," J. Opt. Soc. Am. A **2,** 1419 (1985).
8. T. Szoplik and H. H. Arsenault, "Shift and Scale-Invariant Anamorphic Fourier Correlator Using Multiple Circular Harmonic Filters," Appl. Opt. **24,** 3179 (1985).
9. A. Mahalanobis, B. V. K. Vijaya Kumar, and D. Casasent, "Spatial-Temporal Correlation Filter for In-Plane Distortion Invariance," Appl. Opt. **25,** 4466 (1986).
10. H. H. Arsenault and Y. Sheng, "Properties of Circular Harmonic Expansion for Rotation-Invariant Pattern Recognition," Appl. Opt. **25,** 3225 (1986).
11. G. F. Schils and D. W. Sweeney, "Rotationally Invariant Corrlation Filters for Multiple Images," J. Opt. Soc. Am. A **3,** 902 (1986).

NASA *continued from page 218*

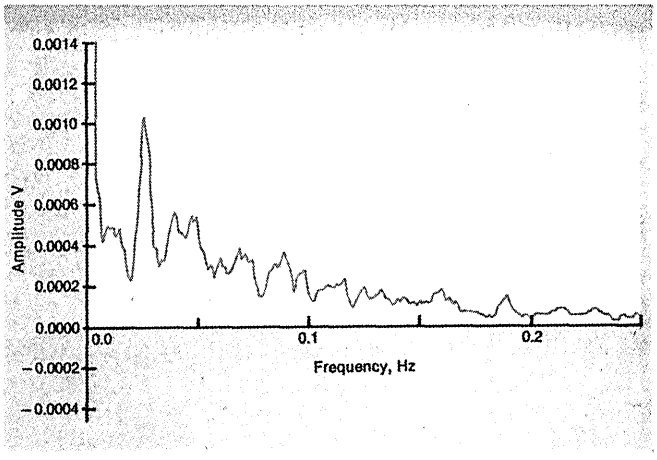

Fig. 7. Fast Fourier transforms of temperature signals indicate the spatial frequencies of striations that have been found in grown crystals.

This technique appears to be a useful procedure to help determine the sources of some growth-induced crystalline defects. The investigation of other processes that may be sensitive to small temperature fluctuations, such as diffusion, precipitation, and corrosion, may also benefit from this technique.

This work was done by Archibald L. Fripp, Jr., Ivan O. Clark, and William J. Debnam, Jr., of Langley Research Center; Patrick G. Barber of Longwood College; Roger K. Crouch of NASA Headquarters; and Richard T. Simchick of PRC Kentron, Inc. Inquiries concerning rights for the commercial use of this invention should be addressed to the Patent Counsel, G. F. Helfrich, Mail Code 279, Langley Research Center, Hampton, VA 23665. Refer to LAR-13670.

Contactless coupling for power and data

An experimental flat-plate coupling transmits digital data signals and electrical power across a small gap between two modules. Unlike multiple-pin electrical connectors, the two halves of the coupling do not have to be aligned precisely for mating; thus, the coupling concept may be a useful substitute for electrical connectors in equipment that has to be assembled by robots, remote manipulators, or humans working in protective clothing or otherwise restricted in dexterity.

The coupling includes a power transformer operating at a frequency of 20 kHz. Each of the mating modules contains half of the pot shaped core of the transformer and a spiral winding (see Fig. 8). Two versions have been built: one to transfer 100 W of power, the other to transfer 1000 W. The transformer is designed to operate at maximum efficiency with a gap of 0.25–0.5 mm between the halves of the core. This eliminates the need to force the halves into contact and thereby also minimizes wear of the mating surfaces. The 100-W version of the transformer has been tested for its performance with various gaps, lateral displacements, and angular misalignments. Within the tolerance range, the transformer exhibits an efficiency as high as 97%.

The data-transmission system includes light-emitting diode transmitters, positive/intrinsic/negative (PIN) diode receivers, and Motorola (or equivalent) emitter-coupled-logic supporting electronic circuitry. The transmitting and receiving diodes are equipped with lenses that give some divergence to the transmitted light beam and field of view, respectively. Consequently, the digital signal coupling also has some tolerance to separations and misalignments. The data transmission system has been tested with a 50-MHz signal representative of a 100-Mbit/s nonreturn-to-zero pulse code.

This work was done by John C. Moody and Joseph W. Foley of OAO Corp. for Goddard Space Flight Center. Refer to GSC-13059.

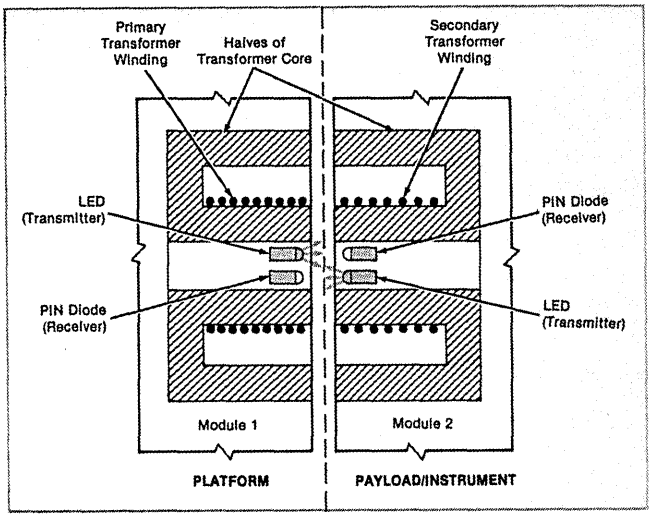

Fig. 8. Split transformer and optoelectronic components transmit electrical power and digital signals, respectively, across a small gap. This coupling would be useful in robotically assembled equipment because it tolerates some misalignment. The coupling also offers higher reliability due to one overall alignment mechanism as opposed to multiple pin/socket alignment requirements.

continued on page 257